10492 *Biochemistry* **2009,** *48,* 10492–10498
DOI: 10.1021/bi9010368

BIOCHEMISTRY
including biophysical chemistry & molecular biology
Article

Single-Molecule Dynamics of the DNA−*Eco*RII Protein Complexes Revealed with High-Speed Atomic Force Microscopy[†]

Jamie L. Gilmore,[‡] Yuki Suzuki,[§] Gintautas Tamulaitis,[∥] Virginijus Siksnys,[∥] Kunio Takeyasu,[§] and Yuri L. Lyubchenko*[,‡]

[‡]*Department of Pharmaceutical Sciences, University of Nebraska Medical Center, 986025 Nebraska Medical Center, Omaha, Nebraska 68198-6025,* [§]*Graduate School of Biostudies, Kyoto University, Yoshida-konoe-cho, Sakyo-ku, Kyoto 606-8502, Japan, and* [∥]*Institute of Biotechnology, Graiciuno 8, Vilnius LT-02241, Lithuania*

Received June 18, 2009; Revised Manuscript Received September 15, 2009

ABSTRACT: The study of interactions of protein with DNA is important for gaining a fundamental understanding of how numerous biological processes occur, including recombination, transcription, repair, etc. In this study, we use the *Eco*RII restriction enzyme, which employs a three-site binding mechanism to catalyze cleavage of a single recognition site. Using high-speed atomic force microscopy (HS-AFM) to image single-molecule interactions in real time, we were able to observe binding, translocation, and dissociation mechanisms of the *Eco*RII protein. The results show that the protein can translocate along DNA to search for the specific binding site. Also, once specifically bound at a single site, the protein is capable of translocating along the DNA to locate the second specific binding site. Furthermore, two alternative modes of dissociation of the *Eco*RII protein from the loop structure were observed, which result in the protein stably bound as monomers to two sites or bound to a single site as a dimer. From these observations, we propose a model in which this pathway is involved in the formation and dynamics of a catalytically active three-site complex.

The formation of synaptic protein−DNA complexes is central to many biological processes that require communication between two or more DNA regions, including recombination (*1*, *2*), replication (*3*), transcriptional regulation (*4*), repair (*5*), transposition (*6*), and restriction (*7*, *8*). Restriction enzymes serve as useful models in the study of mechanisms by which the intracellular protein machinery functions on DNA, including synapsis. Restriction enzymes (REases), which require binding to two or more cognate recognition sites to be catalytically active, are widely spread (*9*). A multisite mechanism suggests that restriction enzymes serve as evolutionary precursors to many DNA regulatory factors in the cell (*10*, *11*). Such a mechanism could also serve an inhibitory function to prevent rare unmethylated recognition sites in the host genome from undergoing restriction (*12*). In addition to systems involving interactions of two DNA helices, interactions of three or more DNA molecules may occur (*13*−*17*).

*Eco*RII is a dimer that recognizes the 5′-CCWGG-3′ sequence. It is generally known as a type IIE restriction enzyme. In general, the definition of type IIE REases is that they bind two DNA recognition sites to cleave one of the sites (*18*). However, recent evidence suggests that the *Eco*RII protein actually requires three sites to concertedly cleave both strands of one recognition site. This formation of a triple synaptic complex (TSC)[1] or two-loop complex was proposed on the basis of kinetic studies with a plasmid containing three recognition sites, which showed that concerted cleavage of a single site occurred much more quickly than with a one-site fragment (*19*). In addition, direct AFM imaging of the complexes confirmed that the *Eco*RII protein and a DNA fragment containing three sites could form TSCs (*8*). The model proposed on the basis of the crystal structure suggests that this occurs by an autoinhibition mechanism (*12*, *20*). The noncatalytic N-terminal binding domains occupy the catalytic C-terminal domain in the unbound protein. For DNA to interact with the catalytic site, the N-terminal sites must first bind to a DNA recognition site and undergo a conformational change to expose the catalytic site of the protein for binding.

There is much interest in how site specific proteins search for their cognate recognition site on DNA. It has been shown that proteins are able to "find" their recognition site 100−1000 times faster than what would be expected for random diffusion using a two-step binding process where the protein first interacts nonspecifically with DNA and then undergoes a translocation process to its specific binding sequence (*21*). In 1981, Berg, Winter, and von Hippel proposed mathematical models of four possible site search mechanisms: macroscopic dissociation−reassociation (random collision), microscopic dissociation−reassociation (hopping), intersegmental transfer, and sliding (*22*, *23*). Various approaches utilizing both bulk techniques (*24*−*26*) and single-molecule techniques (*27*−*29*) have been applied to determine the translocation mechanisms employed by different proteins. Total internal reflection fluorescence microscopy (TIRFM) studies that have been popular for studying translocation of protein along DNA

[†]The work was supported in part by Grant GM 062235 (National Institutes of Health), Grant PHY 0615590 [National Science Foundation (NSF)], the Nebraska Research Initiative (all to Y.L.L.); Grant 0812853 (NSF EAPSI program) and a structural biology and biophysics fellowship to J.L.G. provided by GAANN funding (U.S. Department of Education Grant P200A060150); a Grant-in-aid for Scientific Research (A) (19207001) and Priority Areas (16084203) to K.T.; and a Grant-in-Aid for JSPS Fellows (21-5533) to Y.S.

*To whom correspondence should be addressed: Department of Pharmaceutical Sciences, University of Nebraska Medical Center, 986025 Nebraska Medical Center, Omaha, NE 68198-6025. Phone: (402) 559-5320. Fax: (402) 559-9543. E-mail: ylyubchenko@unmc.edu.

[1]Abbreviations: HS-AFM, high-speed atomic force microscopy; TSC, triple synaptic complex; TIRFM, total internal reflection fluorescence microscopy.

 Published on Web 09/30/2009

(reviewed in ref *30*). This technique is useful because it allows for the direct visualization of a fluorescently labeled protein moving along the DNA; however, the DNA is stretched prior to experiments, which may cause some limitations in what events can be seen. For instance, intersegmental transfer mechanisms that require the formation of DNA loops for the protein to be transferred to another site on the DNA would be problematic to observe with this technique.

For this study, we used high-speed atomic force microscopy (HS-AFM) to directly image single-molecule dynamics of the protein−DNA complexes formed by the *Eco*RII restriction enzyme. It has been used previously to visualize looping and translocation mechanisms of the type III restriction enzyme EcoP15I (*31*). This HS-AFM relies on a small cantilever design based on the original design by Ando (*32*). This technique has the ability to observe molecular dynamics on a time scale that is 100 times faster than that of conventional AFM technology (*31*). On average, we collected images at a rate of two frames per second. With this experimental setup, we observed dynamics of specifically bound looped *Eco*RII complexes. We were able to observe *Eco*RII dissociation, interaction, and translocation. We observed that the protein can dissociate from a loop in two ways, resulting in stable binding of a dimer to a single site or of a monomer bound to each site. Also, the protein could be observed translocating along nonspecific DNA from one region to another. In addition, the complex was seen to move from one specifically bound looped complex to another site, revealing a possible translocation mechanism by which the protein may bind specifically to one site and then bind nonspecifically to the second strand and translocate along the DNA to form the looped complex specifically bound at two sites. The observation of these events helps us to develop a model of how the protein moves along and interacts with DNA to conduct its catalytic functions and also demonstrates the utility of this technique for observing mechanisms of protein−DNA interactions.

METHODS

EcoRII Sample Preparation. The *Eco*RII protein and PCR3 fragment were prepared in the laboratory of V. Siksnys as described previously (*8*). All complexes were assembled in Eppendorf tubes prior to deposition onto a mica surface for imaging. Reaction mixtures contained 1.4 ng/μL PCR3 DNA fragment (810 bp), 3 nM *Eco*RII protein, 40 mM HEPES (pH 8.4), and 5 mM $CaCl_2$ in a total volume of 10 μL. Mg^{2+} ions were replaced with Ca^{2+} ions, which are known to allow binding but prevent cleavage for many restriction enzymes (*33*). The interactions of the DNA are mediated by the Ca^{2+} ions acting as a bridge between the DNA and the negatively charged mica. Reaction mixtures were incubated at ambient temperature for 15 min before 3 μL was deposited onto a 1 mm mica disk for ~1 min and washed with buffer for imaging.

Fast-AFM Imaging. All images were acquired with the HS-AFM microscope in K. Takeyasu's laboratory as described previously (*31*). Scan rates were one to three images per second. For visualization of the complexes without cleavage, the imaging buffer was the same as the binding buffer used to assemble the complexes.

Analysis. All length measurements were taken using the segmented line tool to manually trace the DNA backbone using Image J, free image processing software available from the National Institutes of Health (http://rsb.info.nih.gov/ij/). The AFM scan software in K. Takeyasu's laboratory (*31*) was used to generate the real-time movies, as well as the volume analysis. All volume measurements were taken by measuring the width of the protein in the x plane (a) and in the y plane (b), as well as the height of the protein in the z direction (h). The volume (V) was obtained using the equation for a segment of a sphere (*34*).

$$V = \frac{h\pi}{6}\left(\frac{3ab}{4} + h^2\right)$$

All errors are reported as the standard error of the mean (SEM). Windows Movie Maker was also used extensively for image viewing, as well as for image compression. The supplementary videos and images were rendered in Adobe Photoshop 7.0 to show only the molecule(s) of interest (see Figure S1 of the Supporting Information).

RESULTS

Imaging of EcoRII Complexes. The fragment design used in this experiment is the same as reported previously (*8*) for characterization the three-site binding behavior of the *Eco*RII restriction enzyme in dry AFM images (Figure 1A). This fragment is 810 bp long and contains three recognition sites located almost symmetrically along the DNA fragment. The recognition sites are separated by 283 and 312 bp and are flanked by 100 bp "arms".

A representative image is shown in Figure 1B demonstrating the various types of complexes seen. The *Eco*RII protein can be seen interacting with a single recognition site (i), forming a looped structure with two recognition sites (ii), or forming a double-loop structure interacting with all three sites (iii). These results are in line with previous AFM characterization of *Eco*RII complexes utilizing the same DNA fragment (*8*), which have shown the

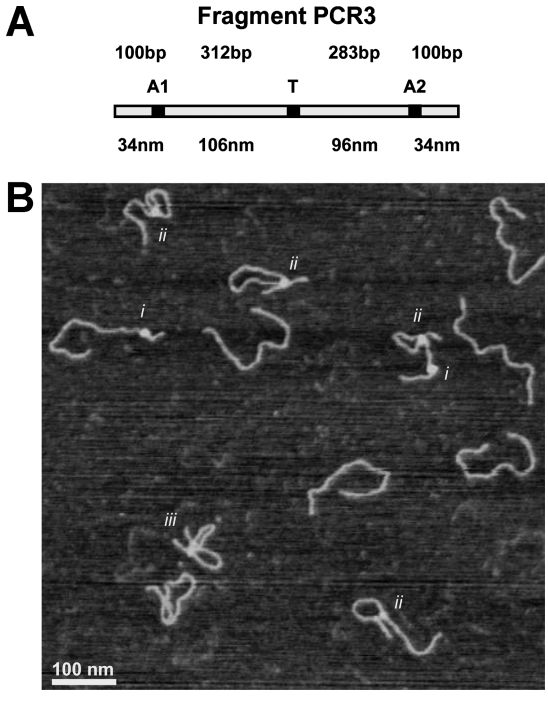

FIGURE 1: Experimental design. (A) PCR3 fragment design showing the location of the three 5 bp *Eco*RII recognition sites along an 810 bp fragment. (B) Types of *Eco*RII DNA complexes in dry AFM images: (i) one-site interactions, (ii) two-site interactions, and (iii) three site interactions.

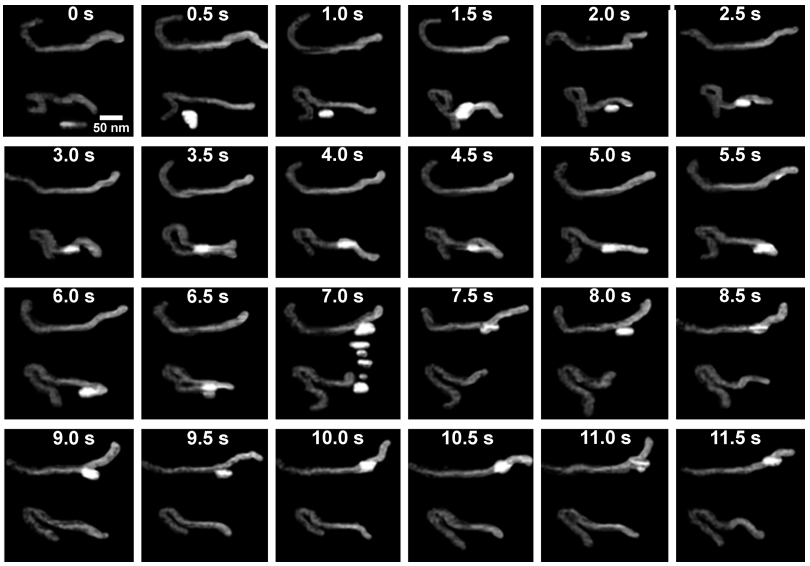

FIGURE 2: *Eco*RII translocation. Consecutive frames of the movement of *Eco*RII over DNA with a time resolution of 500 ms. The protein is seen to bind and form loops. In addition, the protein is seen to bind apparent nonspecific regions of the DNA and translocate down the DNA (from 5.0 to 6.0 s and from 7.5 to 11.5 s). The protein is seen to "come away" from and rebind the protein (8.0 and 9.5 s). Macrohopping to an adjacent DNA strand is seen as well (7.0 s). The smearing effect is due to the raster scan pattern of the microscope in which the tip is tracking the protein as it moves. This event can be seen in video 1 of the Supporting Information.

occurrence of one-site complexes (43%), two-site complexes (55%), and three-site complexes (2%).

Dynamic EcoRII−DNA Interactions. Next, the protein was imaged under aqueous buffer conditions to obtain dynamic images of *Eco*RII−DNA interactions. Figure 2 displays 24 frames acquired at a rate of two frames per second, demonstrating various aspects of the complex dynamics. Video 1 of the Supporting Information also displays this event. Two instances of protein translocation can be seen in this event, first from 4 to 6 s and then from 7 to 11.5 s. Although the protein is seen to "track" the DNA, it appears to follow an interesting path where it is seen to completely overlap the DNA in some frames (as seen at 10−10.5 s) but lie next to the DNA fragment in other frames (as seen at 9−9.5 s). In addition, the protein appeared to briefly interact with two sites to form a transient loop also, as can be seen at 3.5 s and at 6.5 s. At 7 s, the protein can be seen to transfer to another DNA fragment. Multiple blips of the protein motion can be observed in this frame due to the raster scan pattern of the tip, in which the protein is moving toward the other fragment as the tip is scanning, causing the protein to be captured multiple times in the same image. The contribution of the tip to the structure and dynamics of the molecules is impossible to eliminate. However, in this particular case, the protein translocation occurred in the direction perpendicular to the scanning direction. Therefore, the observed dynamics very likely relate to the protein translocation rather than the protein motion exerted by the scanning tip. More examples of one-dimensional diffusion can be observed in Figure S2 and videos 1−5 of the Supporting Information.

In addition to simple translocation of the protein interacting with a single DNA site, translocation was observed on looped DNA as well. The protein remains bound at one recognition site, while the adjacent strand is observed to gradually translocate from one recognition site to another. Figure 3A displays eight frames of this event spanning 20 s. The full event, imaged at a rate of two frames per second, can be observed in video 6 of the Supporting Information. To verify that the protein was interacting with its specific binding sites, the changes in loop, arms, and contour length were measured over time (Figure 3B).

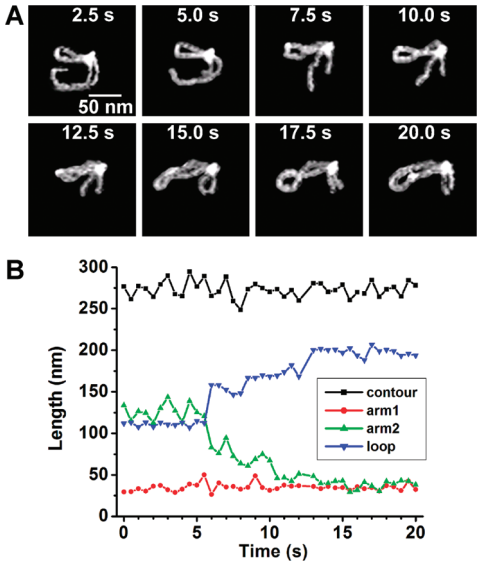

FIGURE 3: *Eco*RII translocation. (A) Individual frames are shown every 2.5 s. Video 6 of the Supporting Information shows this event at two frames per second. (B) Change in DNA length over a time period of 20 s measured in 0.5 s intervals. As the long arm gradually becomes shorter, the loop length gradually increases. The contour lengths of the entire molecule and the short arm have consistent values over the entire time scale. Translocation over the length of 300 bp occurs within 10 s.

The contour length stays close to the expected value of 275 nm for an 810 bp fragment, showing that the dynamics of the molecule do not interfere considerably with the measurements. The short arm 1 also stays at a value close to the expected 34 nm for specific binding 100 bp from the end throughout the imaging period, which shows that the protein remains specifically bound at this recognition site the entire time. The measurements for arm 2 are expected to correspond to either 388 bp (132 nm) or 417 bp (142 nm) when bound at the middle site. This is seen for the most part, although some increased dynamics of the molecule for this arm at the beginning part of the imaging period cause the value to

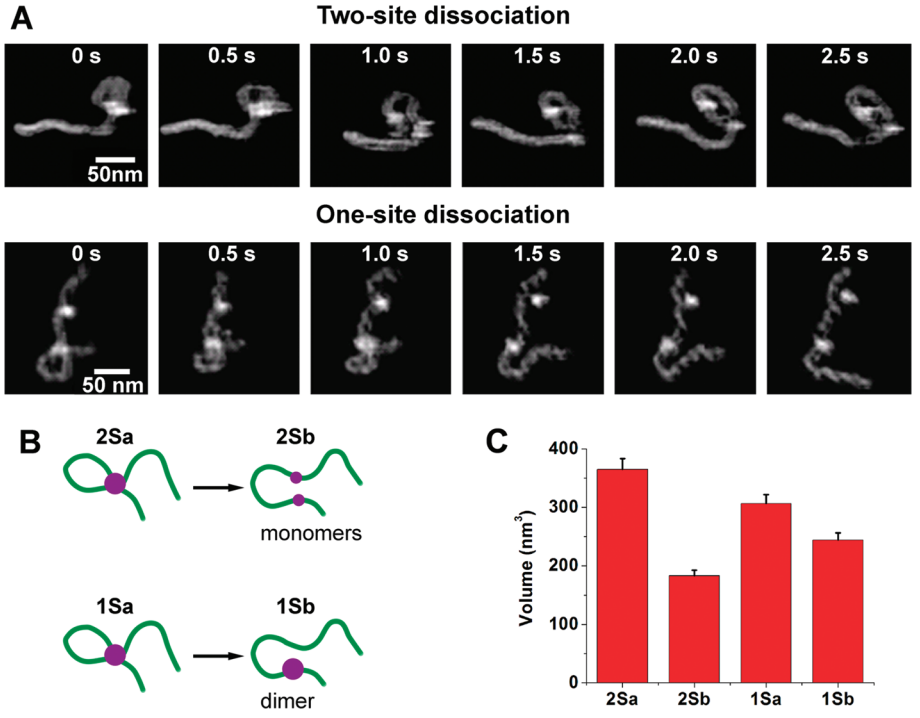

FIGURE 4: *Eco*RII dissociation. (A) Images showing the two modes of dissociation by the *Eco*RII protein, one that results in two protein monomers bound to either site (video 7 of the Supporting Information) and another resulting in a dimer bound to a single site (video 9 of the Supporting Information). (B) Models illustrating the two routes of possible dissociation of the protein with dissociation of the protein into the monomers (top diagram) and without protein dissociation (bottom diagram). (C) Volume analysis for both types of events. For the dissociation to two sites, the protein volume is cut in half, as expected if a dimer is breaking into monomers. For the dissociation to one site, the volume is smaller after dissociation, presumably because there is a contribution of the second DNA strand to the volume measurement.

fall below this value from time to time. These fluctuations are also reflected in the contour length, as many of the "peaks" and "valleys" match, suggesting that the end of the DNA becomes detached from the surface, intermittently causing the DNA to appear shorter. The starting value for the loop also corresponds closely to the expected value for either 283 bp (96 nm) or 312 bp (106 nm). At ~6 s, the loop length begins to increase as the arm length decreases, showing translocation occurs along one arm of the DNA. After 10 s, translocation stops with the protein bound at another specific DNA site. This is validated by the length measurements which show that arm 2 stops at the expected length of 34 nm expected for binding 100 bp from the end, and that the loop stops at the expected value of 207 nm which corresponds to the large 610 bp loop. The change in the loop length occurs over a period of ~10 s covering a distance of ~300 bp (102 nm) until is stops at another recognition site. This means translocation occurs at a rate of ~30 bp/s (10.2 nm/s).

EcoRII Dissociation. For the next portion of the analysis, the dissociation of the *Eco*RII protein from the DNA was examined. For the dissociation of single-loop complexes, we observed that there were two distinct modes of dissociation (Figure 4A and videos 7−10 of the Supporting Information). A model is shown in Figure 4B demonstrating the two pathways, resulting in either a dimer or two monomers which stably interact with a single site. Of 31 observed loop dissociation events, 18 complexes (58%) were seen to dissociate to an intermediate complex interacting with a single site, and 13 complexes (42%) were seen to dissociate by the breaking apart of protein subunits, resulting in a subunit left interacting with both sites.

To gain further insight into the protein stoichiometry in the dissociated complexes, the volume was measured before and after loop dissociation (Figure 4C). The dissociation to two site-bound complexes resulted in an average volume that was approximately half of the volume (183.2 ± 19.0 nm^3) of the predissociation complex (365.1 ± 29.9 nm^3), providing evidence that the protein is, in fact, dissociating into its constituent subunits. When the protein dissociates to bind one site, there is also a slight reduction in volume (244.0 ± 20.1 nm^3) from the predissociation complex (306.5 ± 28.5 nm^3), which could reflect the loss of the contribution of the second DNA strand to the volume of the complex.

In addition to single-loop complexes, 13 double-loop complexes were observed to dissociate (Figure 5 and videos 11 and 12 of the Supporting Information). Of those 13 events, six (46%) dissociated to a small loop, four (31%) dissociated to a large loop, and two (15%) seemed to spontaneously dissociate without a looped intermediate. In the last event of video 2 of the Supporting Information, the two-loop complex actually appeared to dissociate into a big loop and then possibly re-form into the two-loop complexes once again and then dissociate to a small loop intermediate (see Figure S4 of the Supporting Information). These results show that two-site binding is an intermediate complex formed during the dissociation process. Furthermore, it also shows no clear geometrical bias for the mode of double-loop dissociation.

DISCUSSION

With HS-AFM, we have demonstrated the visualization of single-molecule *Eco*RII−DNA complex dynamics at nanoscale. One important finding is that the protein can perform the search for a second cognate site on the DNA while being bound to the first recognition site. This is an expected property of proteins that can bind to several recognition sites but has never been observed directly. The results obtained here also suggest that translocation

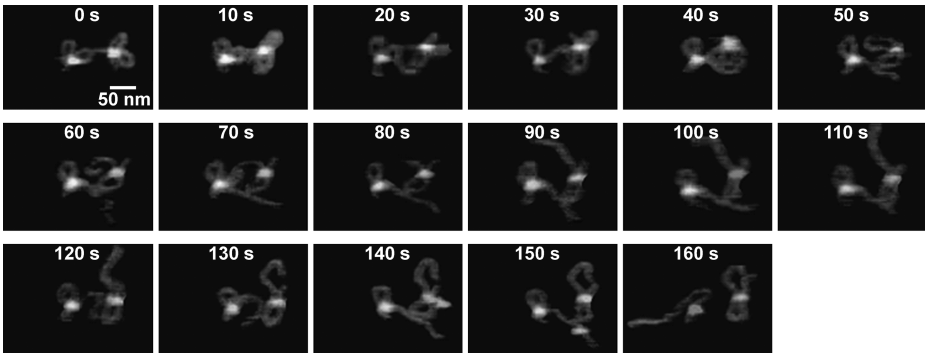

FIGURE 5: Frames showing two-loop dissociation every 10 s. The triple synaptic complex (TSC) at the left dissociates to a single loop at 20 s, followed by the TSC on the right dissociating to a single loop at 50 s. At 160 s, the loop on the left dissociates to a one-site complex. These events, originally imaged at two frames per second, can be seen as movies in video 11 of the Supporting Information.

along the DNA strand by either sliding or hopping mechanisms in search of the initial binding site and the second binding site. The current view of search mechanisms suggests that the optimal route for the protein to quickly locate its target site involves a combination of short-range slides and hops with long-range jumps (*35*). One study using computer simulations came to the conclusion that the most efficient search occurs when a protein is sliding along DNA 20% of the time, and hopping and jumping for the other 80% of the time (*36*). Generally, hopping over DNA is considered to occur in increments of < 10 bp (< 3.4 nm) (*35*). These small-scale dissociation−reassociation events are difficult to observe with the resolution limits of HS-AFM which usually ranges from ~5 to ~10 nm. Although the resolution limits make it difficult to make any definitive conclusions about the degree of hopping or sliding employed by this protein, comparison to a previous HS-AFM study using the same imaging system for the ATP-dependent type III restriction enzyme EcoP15I shows that the protein translocates over the DNA for long distances resulting in accumulated supercoiling (*31*). In contrast, the *Eco*RII protein translocated along the DNA for an average distance of 74 nm (218 bp), ranging from 47 nm (138 bp) to 128 nm (376 bp) before dissociating from the DNA. This value is slightly larger than the previously suggested value of 100 bp (*37*) but is within reason because translocations over shorter distance may have been missed because of the time resolution of the microscope. If translocation occurred over 1−2 s, this event would last four frames or fewer, which makes it difficult to identify events that might have occurred on shorter time scales. Similar HS-AFM studies with different DNA-binding proteins may improve our understanding of how proteins utilizing various search mechanisms behave during the imaging process.

It is interesting to consider how fast the protein is moving along the DNA. From our images, the Einstein equation yields values of 7.2×10^{-4} $\mu m^2/s$ for one-dimensional diffusion and $\sim 1.8 \times 10^{-5}$ $\mu m^2/s$ for two-dimensional diffusion (Figure S3 of the Supporting Information). The protein movement was obviously impaired for two-dimensional diffusion due to interactions with the surface, but the influence of the surface or the tip is not clear. A previous study using the same imaging system attempted to vary the scan rate to see if there was an effect on the measured diffusion rates and found that the diffusion coefficients obtained were not significantly changed (*38*). Currently, TIRF studies are the standard technique for the measurement of diffusion coefficients, but the measurement of looped translocations cannot be performed with such a technique because the DNA must be stretched over the surface (*30*, *39*).

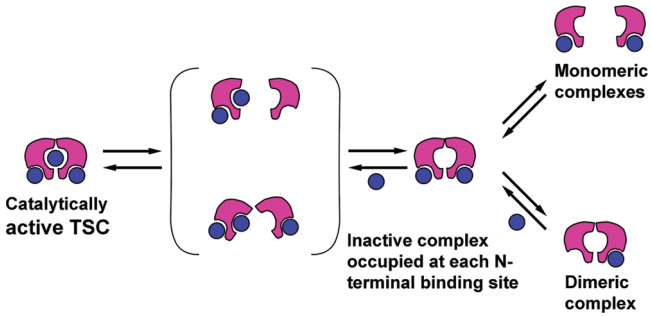

FIGURE 6: Dynamic model of the catalytically active triple synaptic complex (TSC). Circles in this scheme denote the DNA capable of binding to one of the three binding sites of the protein. An active TSC complex is formed after the two N-terminal binding sites are occupied, and the third strand binds to C-terminal pocket. The scheme in brackets shows hypothetical transient forms of the TSC complex illustrating that the complex can dissociate and re-form with or without protein dissociation. The latter pathway is in line with available crystallographic data, whereas the first pathway is consistent with the AFM volume measurements (*8*). The TSC complex breaks apart into two-site complexes followed by the dissociation into two monomeric complexes or a dimeric complex bound to a single binding site.

In this study, *Eco*RII was shown to have two distinct dissociation pathways resulting in either a dimer or two monomers, which remain stably bound to a single site following dissociation of the complexes. These observations support our previous assumption based on imaging of a bilobed shape of the protein in some looped complexes (*8*) and are in line with the results of gel shift experiments (*40*, *41*). These observations prompted us to propose the following model of formation of the *Eco*RII−DNA complex and dynamics (Figure 6). The catalytically active triple synaptic complex loses one contact, resulting in one-loop complexes bound at two recognition sites. We did not find a preference for either possible arrangement of the loops as both small and large loops were observed. In this scenario, the looped complex is shown bound to the N-terminal regions of the protein dimer, but we cannot exclude binding to N- and C-termini. The final step has two possible outcomes that were both observed in our AFM images. Either the protein dissociates from one site with the dimer being bound to the other site, or the dimer can fall apart, forming monomeric complexes. Interestingly, free protein is primarily a dimer in solution (*42*), suggesting that dissociation into monomers is promoted by the protein−DNA interaction. The dissociation of the TSC may proceed via intermediate states shown in brackets. The crystal structure shows that the noncatalytic N-terminal domains block binding to the catalytic

C-terminal domain in the native unbound crystal structure (*20*). If the two N-terminal domains are able to bind two strands, which subsequently break apart into monomers, this may expose the C-terminal site for binding. The third strand may then bind, and the structure may then reassociate to form the active dimeric complex. The association of half-complexes to form the active synaptic complexes is reminiscent of the mechanisms utilized by restriction enzymes SgrA1 (*43*, *44*) and FokI (*45*). An alternative is the dissociation−reassociation method of the third strand via opening of the cleft, which has been proposed previously (*19*). In this scenario, the formation of monomers may simply be a result of dissociation, and not directly observed as an intermediate for complex formation. The first model may lead to the formation of the looped complex mediated by a protein monomer. We did not directly observe these intermediates, so the model of the opening of the cleft for grabbing or dissociation of the third strand is still possible.

In summary, this study demonstrates the power of HS-AFM for the study of protein−DNA interactions. This technique demonstrates the ability to image multisite protein−DNA complexes with DNA in a relaxed conformation not amenable to other methods such as TIRF imaging techniques.

ACKNOWLEDGMENT

We thank L. Shlyakhtenko and A. Lushnikov for the help in preparations for the HS-AFM experiments and useful comments on the manuscript.

SUPPORTING INFORMATION AVAILABLE

Additional images and movies demonstrating protein translocation and dissociation events, in addition to data relating to the calculation of diffusion constants are provided. This material is available free of charge via the Internet at http://pubs.acs.org.

REFERENCES

1. Swanson, P. (2004) The bounty of RAGs: Recombination signal complexes and reaction outcomes. *Immunol. Rev. 200*, 90–114.
2. Mouw, K., Rowland, S., Gajjar, M., Boocock, M., Stark, W., and Rice, P. (2008) Architecture of a serine recombinase-DNA regulatory complex. *Mol. Cell 30*, 145–155.
3. Moens, P., Marcon, E., Shore, J., Kochakpour, N., and Spyropoulos, B. (2007) Initiation and resolution of interhomolog connections: Crossover and non-crossover sites along mouse synaptonemal complexe. *J. Cell Sci. 120*, 1017–1027.
4. Hoverter, N., and Waterman, M. (2008) A Wnt-fall for gene regulation: Repression. *Sci. Signaling 1*, 43.
5. Weterings, E., and Chen, D. (2008) The endless tale of non-homologous end-joining. *Cell Res. 18*, 114–124.
6. Vaezeslami, S., Sterling, R., and Reznikoff, W. (2007) Site-directed mutagenesis studies of tn5 transposase residues involved in synaptic complex formation. *J. Bacteriol. 189*, 7436–7441.
7. Lushnikov, A., Potaman, V., Oussatcheva, E., Sinden, R., and Lyubchenko, Y. (2006) DNA strand arrangement within the SfiI-DNA complex: Atomic force microscopy analysis. *Biochemistry 45*, 152–158.
8. Shlyakhtenko, L., Gilmore, J., Portillo, A., Tamulaitis, G., Siksnys, V., and Lyubchenko, Y. (2007) Direct visualization of the EcoRII-DNA triple synaptic complex by atomic force microscopy. *Biochemistry 46*, 11128–11136.
9. Halford, S., Welsh, A., and Szczelkun, M. (2004) Enzyme-mediated DNA looping. *Annu. Rev. Biophys. Biomol. Struct. 33*, 1–24.
10. Mucke, M., Kruger, D., and Reuter, M. (2003) Diversity of type II restriction endonucleases that require two DNA recognition sites. *Nucleic Acids Res. 31*, 6079–6084.
11. Mucke, M., Grelle, G., Behlke, J., Kraft, R., Kruger, D., and Reuter, M. (2002) EcoRII: A restriction enzyme evolving recombination functions. *EMBO J. 21*, 5262–5268.
12. Szczepek, M., Mackeldanz, P., Moncke-Buchner, E., Alves, J., Kruger, D., and Reuter, M. (2009) Molecular analysis of restriction endonuclease EcoRII from *Escherichia coli* reveals precise regulation of its enzymatic activity by autoinhibition. *Mol. Microbiol. 72*, 1011–1021.
13. Watson, N., and Chaconas, G. (1996) Three-site synapsis during Mu DNA transposition: A critical intermediate preceding engagement of the active site. *Cell 85*, 435–445.
14. Kobryn, K., Watson, M., Allison, R., and Chaconas, G. (2002) The Mu three-site synapse: A strained assembly platform in which delivery of the L1 transposase binding site triggers catalytic commitment. *Mol. Cell 10*, 659–669.
15. Merickel, S., Haykinson, M., and Johnson, R. (1998) Communication between Hin recombinase and Fis regulatory subunits during coordinate activation of Hin-catalyzed site-specific DNA inversion. *Genes Dev. 12*, 2803–2816.
16. Heichman, K., Moskowitz, J., and Johnson, R. (1991) Configuration of DNA strands and mechanism of strand exchange in the Hin invertasome as revealed by analysis of recombinant knots. *Genes Dev. 5*, 1622–1634.
17. Merickel, S., and Johnson, R. (2004) Topological analysis of Hin-catalysed DNA recombination in vivo and in vitro. *Mol. Microbiol. 51*, 1143–1154.
18. Roberts, R., Belfort, M., Bestor, T., Bhagwat, A., Bickle, T., Bitinaite, J., Blumenthal, R., Degtyarev, S., Dryden, K., Dybvig, K., Firman, K., Gromova, E., Gumport, R., Halford, S., Hattman, S., Heitman, J., Hornby, D., Janulaitus, A., Jeltsch, A., Josephsen, J., Kiss, A., Klaenhammer, T., Kobayashi, I., Kong, H., Kruger, D., Lacks, S., Marinus, M., Miyahara, M., Morgan, R., Murray, N., Nagaraja, V., Piekarowicz, A., Pingoud, A., Raleigh, E., Rao, D., Reich, N., Repin, V., Selker, E., Shaw, P., Stein, D., Stoddard, B., Szybalski, W., Trautner, T., VanEtten, J., Vitor, J., Wilson, G., and Xu, S. (2003) A nomenclature for restriction enzymes, DNA methyltransferases, homing endonucleases and their genes. *Nucleic Acids Res. 31*, 1805–1812.
19. Tamulaitis, G., Sasnauskas, G., Mucke, M., and Siksnys, V. (2006) Simultaneous binding of three recognition sites is necessary for a concerted plasmid DNA cleavage by EcoRII restriction endonuclease. *J. Mol. Biol. 358*, 406–419.
20. Zhou, X., Wang, Y., Reuter, M., Mucke, M., Kruger, D., Meehan, E., and Chen, L. (2004) Crystal structure of type IIE restriction endonuclease EcoRII reveals an autoinhibition mechanism by a novel effector-binding fold. *J. Mol. Biol. 335*, 307–319.
21. Riggs, A., Bourgeois, S., and Cohn, M. (1970) The lac repressor-operator interaction. 3. Kinetic studies. *J. Mol. Biol. 53*, 401–417.
22. Berg, O., Winter, R., and von Hippel, P. (1981) Diffusion-Driven Mechanisms of protein Translocation on Nucleic Acids. 1. Models and Theory. *Biochemistry 20*, 6929–6948.
23. Winter, R., and von Hippel, P. (1981) Diffusion-Driven Mechanisms of protein Translocation on Nucleic Acids. 2. The *Echerichia coli* repressor-Operator Interaction: Equilibrium Measurements. *Biochemistry 20*, 6948–6960.
24. Stanford, N., Szczelkun, M., Marko, J., and Halford, S. (2000) One- and three-dimensional pathways for proteins to reach specific DNA sites. *EMBO J. 19*, 6546–6557.
25. Gowers, D., and Halford, S. (2003) Protein motion from non-specific to specific DNA by three-dimensional routes aided by supercoiling. *EMBO J. 22*, 1410–1418.
26. Gowers, D., Wilson, G., and Halford, S. (2005) Measurement of the contributions of 1D and 3D pathways to the translocation of a protein along DNA. *Proc. Natl. Acad. Sci. U.S.A. 102*, 15883–15888.
27. Guthold, M., Zhu, X., Rivetti, C., Yang, G., Thomson, N., Kasas, S., Hansma, H., Smith, B., Hansma, P., and Bustamante, C. (1999) Direct observation of one-dimensional diffusion and transcription by *Escherichia coli* RNA polymerase. *Biophys. J. 77*, 2284–2294.
28. Sakata-Sogawa, K., and Shimamoto, N. (2004) RNA polymerase can track a DNA groove during promoter search. *Proc. Natl. Acad. Sci. U.S.A. 104*, 14731–14735.
29. van den Broek, B., Lomholt, M., Kalisch, S., Metzler, R., and Wuite, G. (2008) How DNA coiling enhances target localization by proteins. *Proc. Natl. Acad. Sci. U.S.A. 105*, 15738–15742.
30. Gorman, J., and Greene, E. (2008) Visualizing one-dimensional diffusion of proteins along DNA. *Nat. Struct. Mol. Biol. 15*, 768–774.
31. Crampton, N., Yokokawa, M., Dryden, D., Edwardson, J., Rao, D., Takeyasu, K., Yoshimura, S., and Henderson, R. (2007) Fast-scan atomic force microscopy reveals that the type III restriction enzyme EcoP15I is capable of DNA translocation and looping. *Proc. Natl. Acad. Sci. U.S.A. 104*, 12755–12760.

32. Ando, T., Kodera, N., Takai, E., Maruyama, D., Saito, K., and Toda, A. (2001) A high-speed atomic force microscope for studying biological macromolecules. *Proc. Natl. Acad. Sci. U.S.A. 98*, 12468–12472.
33. Bellamy, S., Kovacheva, Y., Zulkipli, I., and Halford, S. (2009) Differences between Ca^{2+} and Mg^{2+} in DNA binding and release by the SfiI restriction endonuclease: Implications for DNA looping. *Nucleic Acids Res.* DOI 10.1093/nar/gkp569.
34. Henderson, R., Schneider, S., Li, Q., Hornby, D., White, S., and Oberleithner, H. (1996) Imaging ROMK1 inwardly rectifying ATP-sensitive K^+ channel protein using atomic force microscopy. *Proc. Natl. Acad. Sci. U.S.A. 93*, 8756–8760.
35. Halford, S. (2009) An end to 40 years of mistakes in DNA-protein association kinetics? *Biochem. Soc. Trans. 37*, 343–348.
36. Givaty, O., and Levy, Y. (2008) Protein sliding along DNA: Dynamics and Structural Characterization. *J. Mol. Biol. 385*, 108797.
37. Halford, S. E., and Marko, J. F. (2004) How do site-specific DNA-binding proteins find their targets? *Nucleic Acids Res. 32*, 3040–3052.
38. Yokokawa, M., Yoshimura, S., Naito, Y., Ando, T., Yagi, N., Sakai, N., and Takeyasu, K. (2006) Fast-scanning atomic force microscopy reveals the molecular mechanism of DNA cleavage by ApaI endonuclease. *IEE Proc.: Nanobiotechnol. 153*, 60–66.
39. Fazio, T., Visnapuu, M., Wind, S., and Greene, E. (2008) DNA curtains and nanoscale curtain rods: High-throughput tools for single molecule imaging. *Langmuir 24*, 10524–10531.
40. Karpova, E., Kubareva, E., Gromova, E., and Buryanov, Y. (1993) Peculiarities of the binding of restriction endonuclease EcoRII to synthetic DNA duplexes. *Biochem. Mol. Biol. Int. 29*, 113–121.
41. Karpova, E., Kubareva, E., and Shabarova, Z. (1999) A Model of EcoRII Restriction Endonuclease Action: The Active complex is Most Likely Formed by One Protein Subunit and One DNA Recognition Site. *IUBMB Life 48*, 91–98.
42. Reuter, M., Kupper, D., Meisel, A., Schroeder, C., and Kruger, D. (1998) Cooperative Binding Properties of Restriction Endonuclease EcoRII with DNA Recognition Sites. *J. Biol. Chem. 273*, 8294–8300.
43. Wood, K., Daniels, L., and Halford, S. (2005) Long-range communications between DNA sites by the dimeric restriction endonuclease SgrAI. *J. Mol. Biol. 350*, 240–253.
44. Daniels, L., Wood, K., Scott, D., and Halford, S. (2003) Subunit assembly for DNA cleavage by restriction endonuclease SgrAI. *J. Mol. Biol. 327*, 579–591.
45. Bitinaite, J., Wah, D., Aggarwal, A., and Schildkraut, I. (1998) FokI dimerization is required for DNA cleavage. *Proc. Natl. Acad. Sci. U.S.A. 95*, 10570–10575.